ELSEVIER

Journal of Alloys and Compounds 218 (1995) 165–172

Journal of ALLOYS AND COMPOUNDS

Hydrogen-induced magnetic anisotropy and crystal lattice distortion in $Sm_{1-x}Tb_x(Fe_{0.2}Co_{0.8})_2$ compounds

N.V. Mushnikov *, V.S. Gaviko, A.V. Korolyov, N.K. Zajkov

Institute of Metal Physics, 620219 Ekaterinburg, Russia

Received 14 June 1994

Abstract

Induced magnetic anisotropy in $Sm_{1-x}Tb_x(Fe_{0.2}Co_{0.8})_2$ compounds caused by spontaneously absorbed hydrogen was investigated. It is shown that hydrogen-induced anisotropy appears in the compounds with both negative and positive magnetostriction λ and becomes minimal when magnetostriction is near zero. The calculation of magnetocrystalline anisotropy using single ion model in point charge approximation showed that hydrogen occupied AB_3-type interstitial sites rather than A_2B_2. It was found that the ordering of hydrogen causes the additional crystal lattice distortion at $\lambda<0$ but not at $\lambda>0$, which is explained in the framework of the geometrical model by the different anisotropy of hydrogen distribution in the crystal lattice.

Keywords: Induced magnetic anisotropy; Magnetostriction; Hydrogen; Crystal lattice distortions

1. Introduction

It has been shown recently [1–4] that cubic ferromagnetic $Sm(Fe,Co)_2$ compounds absorb a small amount of hydrogen from the atmosphere under normal conditions. These compounds have a ⟨111⟩-type easy axis at room temperature and negative magnetostriction constant λ_{111}. As a result of strong magnetoelastic interactions in the magnetically ordered state, the crystal lattice is "compressed" along the crystallographic [111] axis, along which the spontaneous magnetization vector is aligned. It was assumed [1–4] that such rhombohedral magnetoelastic crystal lattice distortion starts the hydrogen ordering. This in turn results in a sharp increase of the rhombohedral deformation and in the occurrence of a local uniaxial magnetic anisotropy. The orientation of local easy axes is determined by the direction of the magnetoelastic deformation, which can be changed by varying the direction of an applied magnetic field. If the temperature of hydrogen disordering is below the Curie temperature T_c, thermomagnetic treatment of such samples induces a gigantic uniaxial anisotropy with energy E_u up to 2×10^6 J m^{-3}.

The ordering and reordering of hydrogen in such a model are caused by magnetoelastic lattice deformation. Hence it is of interest to study the effect of the value and sign of the initial magnetoelastic lattice deformation on the induced magnetic anisotropy and crystal lattice distortion caused by hydrogen ordering. For this purpose we have prepared $Sm_{1-x}Tb_x(Fe_{0.2}Co_{0.8})_2$ compounds with $0\leqslant x\leqslant 1$. The compound with Tb ($x=1$) is known to have a ⟨111⟩-type easy axis also, but in contrast to Sm compounds, their magnetostriction constant λ_{111} is positive. The large magnetostriction in these compounds is due to rare earth ions [5]. According to the single-ion model, zero-value magnetostriction can be expected at some x content. The relative content of Fe and Co in the alloys was chosen for the following reasons. First, in the $Sm(Fe_{1-y}Co_y)_2$ system at $y<0.5$, the spin-reorientation transition to the ⟨110⟩ easy axis phase takes place at low temperatures [6], which is outside the scope of this investigation. Second, the maximum crystal lattice deformation due to hydrogen ordering was observed at $y=0.8$ [3].

2. Experimental

Polycrystalline samples were obtained by melting constituents in an argon atmosphere. After annealing for 70 h at 750 °C, the amount of secondary phases was not more than 3%. As was shown earlier [1–3], powdered samples absorb hydrogen from the atmosphere more actively than bulk samples, and saturation

* Corresponding author.

SSDI 0925-8388(94)01341-1

is usually achieved in 2–3 weeks. We prepared powdered samples with grain dimensions between 36 and 63 μm. After contact with the atmosphere for 2 months, mass spectrometric investigations showed that the concentration of hydrogen was 3 at.% and the variation for samples with different x was not more than ±0.6 at.%. The hydrogen content in bulk samples is approximately an order of magnitude smaller.

The crystalline structure was investigated using an X-ray diffractometer with Cr Kα radiation. The degree of rhombohedral distortion $\epsilon = \alpha - \pi/2$, where α is the angle at the vertex of the rhombohedron, was determined from the value and the character of splitting of (440) and (222) Bragg reflections in a cubic description. The crystal lattice parameters of the investigated compounds together with the Curie temperatures, determined from the temperature dependence of ac susceptibility, are given in Table 1.

The magnetostriction of bulk polycrystalline samples was measured in magnetic fields up to 2 T in the temperature range 4.2–300 K using strain gauges attached directly to the surface of the sample.

The magnetization and induced magnetic anisotropy were investigated using a vibrating sample magnetometer in magnetic fields up to 2 T in the temperature range 77–550 K. Before magnetic measurements, powdered samples were pressed into disc-shaped pellets 5 mm in diameter and 2 mm thick. The uniaxial magnetic anisotropy was induced by heating of the pellet to 550 K > T_c and then by cooling at a rate of ca. 10 K min^{-1} in a magnetic field of 0.6 T. The energy of induced magnetic anisotropy was determined from the area between the demagnetization curves measured along the axis of the induced anisotropy and perpendicular to it. In order to eliminate the contribution of magnetostatic energy, in both cases the magnetic field was applied in the plane of the pellet.

Table 1
Crystal lattice parameters a and ϵ at 300 K and Curie temperatures T_c of $Sm_{1-x}Tb_xFe_{0.4}Co_{1.6}$ compounds

x	Lattice parameters		T_c (K)
	a (nm)	ϵ (10^{-3} rad)	
0	0.7300	−1.2	430
0.1	0.7297	−0.73	439
0.2	0.7294	−0.58	448
0.3	0.7292	–	453
0.4	0.7288	–	460
0.5	0.7280	–	466
0.6	0.7275	0.29	473
0.7	0.7271	0.48	482
0.8	0.7266	0.82	491
0.9	0.7263	1.21	502
1.0	0.7258	1.60	510

3. Results

In accordance with generally recognized representations, the magnetic moment of $Sm_{1-x}Tb_x(Fe_{0.2}Co_{0.8})_2$ can be written in the form $M = M_{3d} + M_{Sm} - M_{Tb}$, where M_{3d}, M_{Sm} and M_{Tb} are magnetic moments of the 3d sublattice, Sm sublattice (ca. 0.3 μ_B per Sm atom) and Tb sublattice ($\leqslant 9$ μ_B per Tb atom). In both $TbFe_2$ and $TbCo_2$ at any temperature in a magnetically ordered state, $M_{Tb} > M_{3d}$. Therefore, the magnetic compensation temperature can be expected in the investigated system. Fig. 1 shows the temperature dependences of the magnetization in a field $\mu_0 H = 0.6$ T. It can be seen that magnetic compensation is really observed at $0.3 \leqslant x \leqslant 0.4$. However, at the compensation temperature the magnetization does not reach zero, as is evident for $x = 0.36$ (Fig. 1(b)). This result is probably due to the slightly inhomogeneous distribution of Sm and Tb atoms in the sample, which was discussed in detail in previous papers [7,8].

In addition to magnetic compensation, magnetostriction compensation is also observed in this system. Fig. 2 shows the temperature dependences of the magnetostriction $\lambda_{\parallel} - \lambda_{\perp}$, measured in the process of rotation of the sample in a field of 1.5 T. At $x = 0.4$ the magnetostriction is close to zero in a wide temperature range. The low value of the magnetostriction for $x = 0.3$ at $T < 100$ K is probably due to a large value

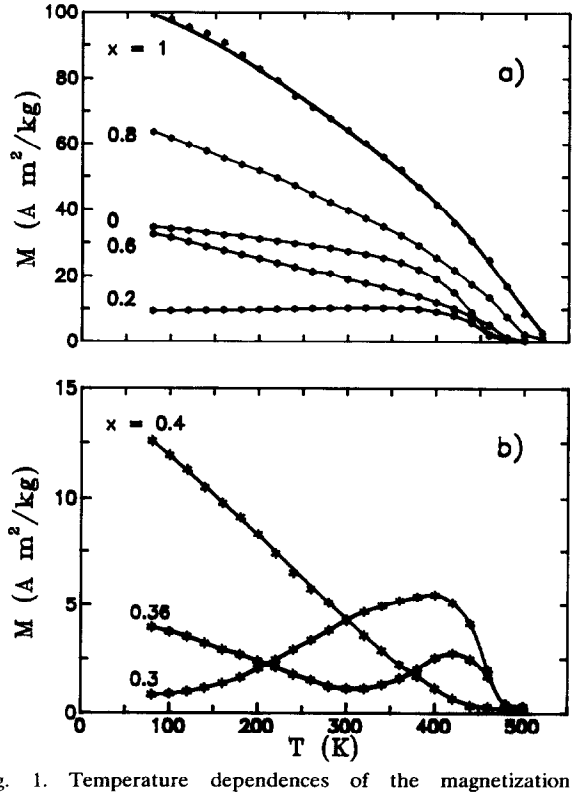

Fig. 1. Temperature dependences of the magnetization of $Sm_{1-x}Tb_x(Fe_{0.2}Co_{0.8})_2$ compounds in a field $\mu_0 H = 0.6$ T.

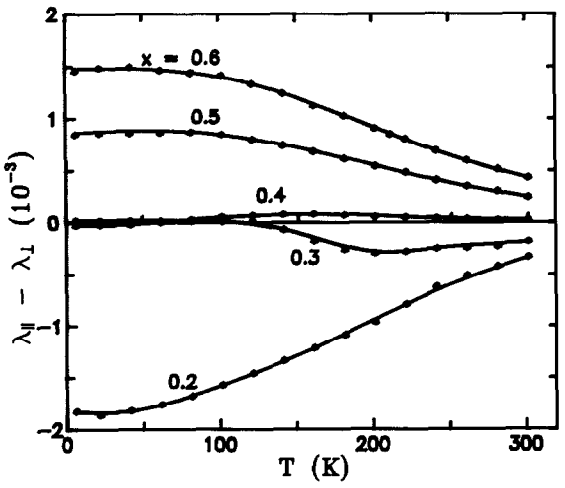

Fig. 2. Temperature dependences of anisotropic magnetostriction $(\lambda_{\parallel} - \lambda_{\perp})$ in a field $\mu_0 H = 1.5$ T for $Sm_{1-x}Tb_x(Fe_{0.2}Co_{0.8})_2$ bulk samples at different x values.

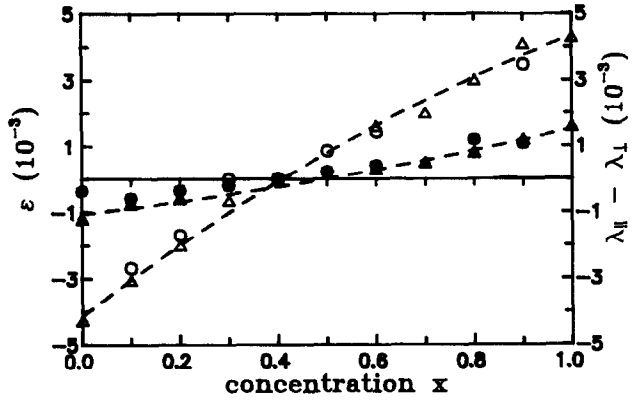

Fig. 3. Concentration dependences of crystal lattice distortion parameter ϵ (triangles) and anisotropic magnetostriction $(\lambda_{\parallel} - \lambda_{\perp})$ (circles) of $Sm_{1-x}Tb_x(Fe_{0.2}Co_{0.8})_2$ compounds at 77 K (open symbols) and 290 K (closed symbols).

of the anisotropy field caused by a small magnetization. As for cubic rare earth intermetallic compounds with a ⟨111⟩-type easy axis $\lambda_{111} \gg \lambda_{100}$ [5], for the saturation magnetostriction of isotropic polycrystal the following relation is valid:

$$\lambda_{\parallel} - \lambda_{\perp} = \frac{3}{2}\lambda_s = \frac{3}{2}\left(\frac{2}{5}\lambda_{100} + \frac{3}{5}\lambda_{111}\right) \approx 0.9\,\lambda_{111} \qquad (1)$$

Hence, for hydrogen-free bulk samples the correlation between $\epsilon = \lambda_{111}$ and $(\lambda_{\parallel} - \lambda_{\perp})$ can be expected. In fact, the concentration dependences of ϵ and $(\lambda_{\parallel} - \lambda_{\perp})$ were found to be similar (Fig. 3). At any temperature these dependences are nearly linear, which is inconsistent with the single-ion nature of the magnetostriction in these compounds.

As was reported earlier [1,2], powdered $Sm(Fe,Co)_2$ samples possess an additional rhombohedral lattice deformation caused by the ordering of hydrogen. When the sample is heated, this deformation disappears in a narrow temperature range near room temperature due to hydrogen disordering. Fig. 4 shows temperature dependences of ϵ for bulk and powdered samples with $x = 0$, 0.1 and 0.2. It is seen that when x increases, both the magnetoelastic deformation (ϵ value for bulk sample) and hydrogen-induced deformation decrease. In addition, the temperature of hydrogen disordering increases. For other compositions no difference in the crystal lattice distortions of either bulk or powdered samples is observed, in spite of the fact that the magnetoelastic deformation of Tb-rich compounds is rather high.

The induced anisotropy effect was observed with powdered samples of all compositions. After cooling in a magnetic field, the demagnetization curves measured along and perpendicular to the field direction in the annealing process differ substantially (Fig. 5). The induced anisotropy energy E_u decreases monotonically with increase in temperature (Fig. 6). and becomes zero at a hydrogen ordering temperature T_k. For all compositions, the variation in T_k does not exceed

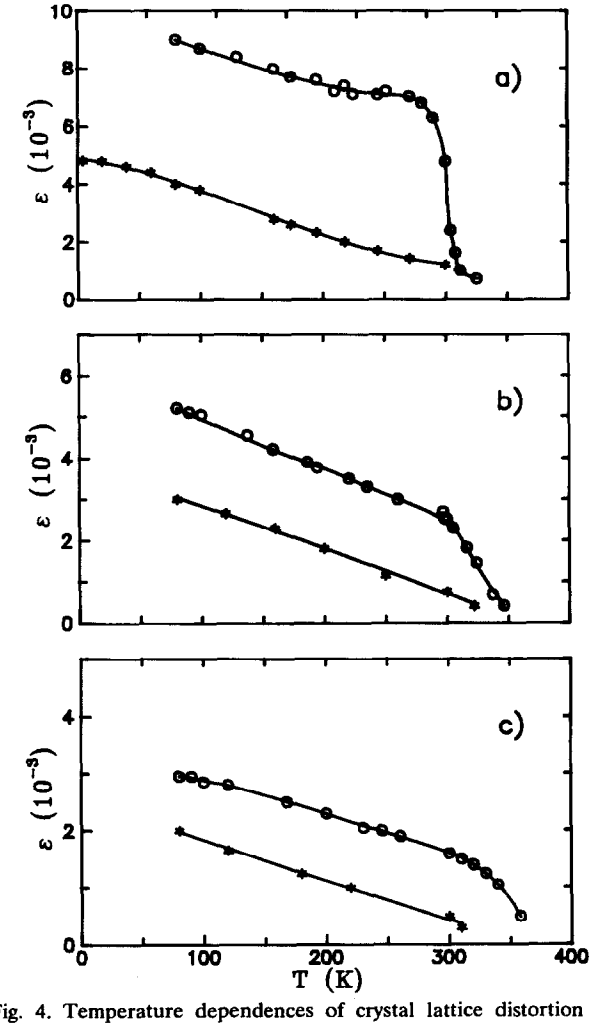

Fig. 4. Temperature dependences of crystal lattice distortion parameter ϵ for (*) bulk and (O) powdered $Sm_{1-x}Tb_x(Fe_{0.2}Co_{0.8})_2$ samples. (a) $x = 0$; (b) $x = 0.1$; (c) $x = 0.2$.

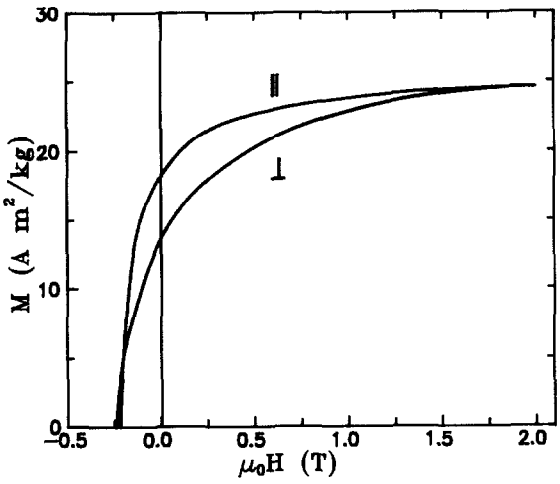

Fig. 5. Demagnetization curves of $Sm_{0.5}Tb_{0.5}(Fe_{0.2}Co_{0.8})_2$ sample at 77 K after heating to 450 K and subsequent cooling in a field of 0.6 T: ∥, measurements along the direction of the field applied during heat treatment; ⊥, measurements perpendicular to it.

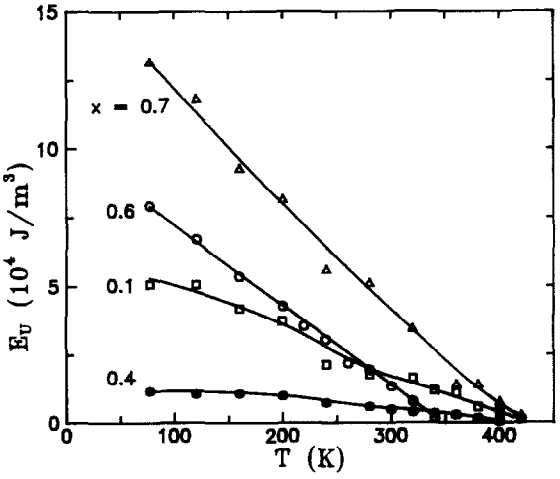

Fig. 6. Temperature dependences of induced magnetic anisotropy of $Sm_{1-x}Tb_x(Fe_{0.2}Co_{0.8})_2$ samples with different x.

25%. As was mentioned previously [3], the T_k value depends on the hydrogen content. In our case, the $T_k(x)$ behaviour correlates with mass spectrometric data on the amount of hydrogen in the samples.

It should be noticed that in the framework of the thermoactivation mechanism of hydrogen diffusion, the T_k characteristic is rather conventional and it means only that at $T > T_k$ the time interval of measuring the magnetization curve exceeds the time of hydrogen reordering.

Fig. 7 shows the concentration dependences of the induced anisotropy energy E_u. Both at 77 K and at 290 K E_u has a minimum near the compositions corresponding to minimal magnetostriction values. This is in agreement with the model of hydrogen ordering under the influence of magnetoelastic lattice deformation. Also, although the magnetic compensation takes place near this concentration too (see Fig. 1), the small

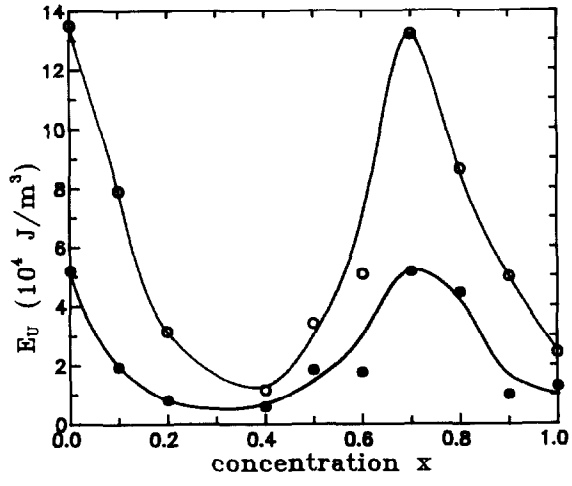

Fig. 7. Concentration dependences of induced magnetic anisotropy of $Sm_{1-x}Tb_x(Fe_{0.2}Co_{0.8})_2$ samples at (○) 77 K and (●) 290 K.

E_u value probably cannot be due to the magnetic compensation, because the $M(H)$ and $\lambda(H)$ dependences for compounds with $x = 0.3$ and 0.4 are close to saturation in the field $\mu_0 H > 1.5$ T at room temperature. At $x = 0.7$, the $E_u(x)$ dependence reaches a maximum and then decreases with increasing x, whereas the magnetoelastic deformation (Fig. 3) continues to increase. Probably for these compositions ($x > 0.7$) hydrogen has no time to order completely during magnetic annealing, because when the magnetoelastic distortion appeared at $T < T_c$, the hydrogen diffusion rate seemed to be low. In fact, the magnetic annealing of $Sm_{0.1}Tb_{0.9}(Fe,Co)_2$ for 8 h at 450 K $< T_c$ leads to an increase in E_u from 1×10^4 to 5.4×10^4 J m^{-3} at room temperature.

4. Discussion

Two mechanisms for the appearance of induced magnetic anisotropy are possible in these compounds. First, the induced anisotropy can be caused by the elastic energy of the lattice, deformed on hydrogen ordering. In this case the constant of induced uniaxial anisotropy is equal to $K_u = (3/2)\lambda_{111}\epsilon_H G$, where G is the shear modulus and $\epsilon_H = \epsilon - \lambda_{111}$ is an additional lattice deformation caused by hydrogen ordering. For $Sm(Fe,Co)_2$ at the typical intermetallics value $G = 10^{11}$ N m^{-2} [5], this gives $K_u \approx 10^6$ J m^{-3}, which is sufficient for explanation of the experimental E_u values. E_u represents the work of magnetization, and $E_u \leqslant K_u$. Substitution of Sm atoms by Tb leads to a change in the magnetostriction sign without a change in the type of induced magnetic anisotropy, which remains uniaxial (K_u is positive). Hence the hydrogen-induced deformation ϵ_H should change its sign. However, in Tb-enriched compounds we did not observe any changes in lattice deformation during hydrogen absorption, i.e., $|\epsilon_H| \leqslant 3 \times 10^{-4}$.

Another mechanism for the appearance of induced magnetic anisotropy is the contribution of hydrogen ions to the magnetocrystalline anisotropy. We used the point-charge model for evaluation of this contribution. First, it is necessary to determine which sites are preferable for hydrogen in the deformed lattice. Hydrogen can occupy two types of tetrahedral interstitial sites in the $MgCu_2$ structure: AB_3 (32e sites) and A_2B_2 (96g sites). Here, in accordance with the notations in Ref. [9], A is an R atom and B denotes a 3d atom. So far no strict evidence has been presented as to which type of site is preferable for hydrogen. There are data about preferable occupation of both AB_3 [10,11] and A_2B_2 interstitials [12,13]. In the case of weak solutions of hydrogen (α-phases), there are no such data. Geometrical calculations also give the maximal size (i.e. the radius of inscribed ball in the model of tightly packed balls) of both AB_3 and A_2B_2 interstitials depending or whether tabulated values of atomic radii or those calculated for real compounds are used [14]. That is why we made estimations for both interstitials. In a non-deformed lattice all interstitial sites of one type are equivalent. After taking into account the magnetoelastic deformation, inequivalency of sites appeared. In Table 2, radii of inscribed balls and the number of interstitials of the given radius are listed for $Tb(Fe,Co)_2$ ($a=0.7258$ nm, $\lambda=0.0016$) and $Sm(Fe,Co)_2$ ($a=0.7300$ nm, $\lambda=-0.0012$). In this calculation we assumed the magnetostriction deformation to be uniform: the projections of atomic coordinates on the [111] direction were multiplied by $(1+\lambda)$, whereas the projections of atomic coordinates on the (111) plane were multiplied by $(1-\lambda/2)$.

It is reasonable to assume that in a distorted lattice hydrogen atoms occupy only interstitials having a maximum size. Coordinates of the centres of such interstitials are presented in Table 3. We do not take into account the exclusion rule [9], which forbids hydrogen from occupying closely placed sites at distances of less than 0.22 nm, because the real concentration of hydrogen in samples (ca. 0.1 H atom per formula unit) is 30 times less than the number of such sites (10 times in the case of AB_3 sites at $\lambda>0$).

In a spherical system of coordinates with the c-axis parallel to the [111] direction, the magnetocrystalline anisotropy energy of both cubic and rhombohedrally deformed samples can be represented as a series on the orthonormal Legendre polynomials:

$$E_a=\sum_{n,m} k_n^m\left[\frac{(n-m)!}{(n+m)!}\right]^{1/2} P_n^m(\cos\theta)\exp(-\phi) \qquad (2)$$

where θ is the angle between the magnetization vector M_s and the c-axis and ϕ is the angle between the projections of M_s and (100) vectors in the (111) plane. The anisotropy coefficients k_n^m are connected with the anisotropy constants K_i of uniaxial crystals by the relations [15]

$$K_1=-\frac{3}{2}k_2^0-5k_4^0-\frac{21}{2}k_6^0,$$

$$K_2=\frac{35}{8}k_4^0+\frac{189}{8}k_6^0 \qquad (3)$$

For a cubic lattice in such system of coordinates,

$$K_1=\frac{15}{2}k_4^0-\frac{189}{32}k_6^0, \qquad K_2=\frac{2079}{32}k_6^0 \qquad (4)$$

In the case where the exchange energy of R–3d is much larger than the crystal electric field (CEF) potentials energy of R ions, Legendre polynomials are classical equivalents of Stevens operators. Therefore, at 0 K the coefficients k_n^m are connected directly to the CEF parameters:

$$k_n^m=\theta_n\langle r^n\rangle\langle O_n^0\rangle A_n^m \qquad (5)$$

where $\theta_2\equiv\alpha_J$, $\theta_4\equiv\beta_J$, $\theta_6\equiv\gamma_J$ are Stevens parameters [16], $\langle r^n\rangle$ is the average of the nth power of the 4f

Table 2
Calculated radius of inscribed ball (r) and the number of interstitial sites of given radius (n) around R atom for alloys with different sign of distortion ϵ [a]

Type of interstitial	$Tb(Fe,Co)_2$ ($a=0.7258$ nm)				$Sm(Fe,Co)_2$ ($a=0.7300$ nm)			
	$\epsilon=0$		$\epsilon=+0.0016$		$\epsilon=0$		$\epsilon=-0.0012$	
	r (nm)	n	r (nm)	n	r (nm)	n	r (nm)	n
AB_3	0.031236	4	0.031229	3	0.031723	4	0.031727	3
			0.031257	1			0.031708	1
A_2B_2	0.029157	24	0.029146	6	0.029271	24	0.029261	6
			0.029156	12			0.029272	12
			0.029172	6			0.029281	6

Metallic radii of Tb, Sm and 3d-atoms were taken as 0.178, 0.180 and 0.126 nm, respectively.

Table 3
Hydrogen site coordinates in the interstitials having maximum size

Compound	Type of interstitial	Position No.	Coordinates		
			x/a	y/a	z/a
$Tb(Fe,Co)_2$	AB_3	1	−0.166	−0.166	−0.166
	A_2B_2	1	−0.049	−0.049	0.277
		2	−0.049	0.277	−0.049
		3	0.277	−0.049	−0.049
		4	−0.201	−0.201	−0.027
		5	−0.201	−0.027	−0.201
		6	−0.027	−0.201	−0.201
$Sm(Fe,Co)_2$	AB_3	1	−0.167	−0.167	0.167
		2	−0.167	0.167	−0.167
		3	0.167	−0.167	−0.167
	A_2B_2	1	0.048	0.048	0.278
		2	0.048	0.278	0.048
		3	0.278	0.048	0.048
		4	0.202	0.202	−0.029
		5	0.202	−0.029	0.202
		6	−0.029	0.202	0.202

shell radius [17] and $\langle O_n^0 \rangle$ are the expectation values of Stevens equivalent operators tabulated in Ref. [16].

Crystal electric field parameters A_n^m in the framework of point charge model can be written as

$$A_n^m(i) = Z_i A_n^m(i) \quad (6)$$

where Z_i are effective charges of i-type ions and Λ_n^m are lattice sums:

$$\Lambda_n^m(i) = \sum_j \frac{1}{r_j^{n+1}} \left[\frac{(n-m)!}{(n+m)!}\right]^{1/2} P_n^m(\cos\theta)\exp(-\phi) \quad (7)$$

where r_j is the distance from atom j to atom R (000) and θ and ϕ are angle coordinates of atom j. The summation includes nearest neighbours of atom R (000).

In Table 4, non-zero values of Λ_n^m for lattices with both positive and negative distortions are given. It is seen that the lattice sums Λ_2^0 for R and M atoms are small (for a cubic lattice $\Lambda_2^0 = 0$). In the case of hydrides, a large Λ_2^0 from hydrogen ions will give the main contribution to the crystal field. Hence in the case of occupation of both AB_3 interstitials and A_2B_2 a strong local uniaxial anisotropy will appear in hydrides.

In order to evaluate the anisotropy constants we need to render the effective charges of ions. It has been shown [18] that the best coincidence of experimental anisotropy constants with those calculated for rare earth intermetallic compounds with different crystal lattices is observed at the values of ion charges $Z_R = 3$, $Z_M = 0.2$. For Laves phase hydrogen-free compounds, our calculations using such charge values give $K_1 = -3.2\times10^7$ J m^{-3} for $TbFe_2$ and -2.1×10^7 J m^{-3} for $ErFe_2$, whereas single-crystal measurements give -7.6×10^7 and -3.6×10^7 J m^{-3}, respectively [5,19]. The hydrogen ion charge was taken as -1. A negative sign of Z_H is generally recognized for M = Fe, and probably there are no changes in sign of Z_H in the $Sm(Fe_{1-y}Co_y)_2$ system [6].

As can be seen from Eq. (3), when the rhombohedral deformation becomes zero, the uniaxial anisotropy con-

Table 4
Lattice sums for rhombohedrally deformed crystal lattices

Compound	Atoms	Λ_2^0 (nm^{-5})	Λ_4^0 (nm^{-5})	Λ_4^3 (nm^{-5})	Λ_6^0 (nm^{-7})	Λ_6^3 (nm^{-7})	Λ_6^6 (nm^{-7})
$Tb(Fe,Co)_2$	R	−0.1368	334.4	405.9	5201	−3157	3311
$\epsilon = 0.0016$	Fe	0.1515	−406.9	−485.8	1617	−879.7	1040
	H(AB_3)	109.2	2493	0	56940	0	0
	H(A_2B_2)	110.0	−59.08	−2170	−23500	119700	58460
$Sm(Fe,Co)_2$	R	0.3592	338.5	388.7	5056	−3009	3156
$\epsilon = -0.0042$	Fe	−0.3908	−394.1	−472.5	1416	−1102	860.8
	H(AB_3)	−105.6	99.03	2907	30144	−50105	52552
	H(A_2B_2)	227.8	−5177	0	−97585	0	13290

stant K_1 does not come to zero owing to the non-zero values of k_4^0 and k_6^0. For this reason we limit ourselves to the first term in Eq. (3), i.e. we take $K_u = -(3/2)k_2^0$. Since the number of H atoms is much less than the number of available sites, the calculated anisotropy constant value for the case of total occupation of maximal size interstitials was multiplied by the relative density of hydrogen (1/10 for AB_3 sites, $\lambda > 0$, and 1/30 for all other cases). The calculated K_u values at 0 K are given in Table 5. It is evident that real K_u values can differ considerably from the values calculated on the basis of the point charge model without taking into account the screening effects. However, it should be noted that as the A_2^0 sum from hydrogen gives the main contribution to K_u, the result of calculation hardly depends on the reasonable changes of R and M charge values. The calculated K_u values are much larger than the experimental E_u values. This may be due to the partial ordering of hydrogen, i.e. H atoms can occupy some of the interstitial sites having smaller dimensions. In any case, the proposed mechanism allows one to explain the observed phenomena of induced anisotropy.

It can be seen from Table 5 that even without taking into account the contribution of H ions to the crystal electric field (i.e. at $Z_H = 0$), the uniaxial magnetic anisotropy constant caused by CEF deformation is positive and has the same order of magnitude as K_u obtained from the evaluation of the energy of an elastically deformed lattice (see above). By taking into account H ion charges we have $K_u > 0$ for AB_3 sites, independent of the sign of magnetostriction, and for A_2B_2 sites $K_u > 0$ when $\lambda > 0$ and $K_u < 0$ when $\lambda < 0$. Special studies showed that anisotropy of the "easy plane" type ($K_u < 0$) is not induced in these compounds. Hence it can be concluded that hydrogen occupied AB_3-type interstitials rather than A_2B_2.

Let us consider possible sites of hydrogen in greater detail. Fig. 8 shows Friauf polyhedra formed by B atoms around an A atom and hydrogen sites in both AB_3 and A_2B_2 interstitials. It is seen that in both cases the distribution of hydrogen is more anisotropic when lattice deformation is negative than with positive deformation,. If hydrogen occupies AB_3 interstitials, at $\epsilon > 0$ each

Table 5
Induced anisotropy constants K_u calculated using point-charge model

Compound	Lattice distortion, ϵ (rad)	$K_u = -(3/2)k_2^0$ (10^7 J m^{-3})
$Tb(Fe,Co)_2$	0.0016	0.194
$Tb(Fe,Co)_2 + H(AB_3)$	0.0016	0.578
$Tb(Fe,Co)_2 + H(A_2B_2)$	0.0016	2.07
$Sm(Fe,Co)_2$	−0.0042	0.362
$Sm(Fe,Co)_2 + H(AB_3)$	−0.0042	1.64
$Sm(Fe,Co)_2 + H(A_2B_2)$	−0.0042	−2.39

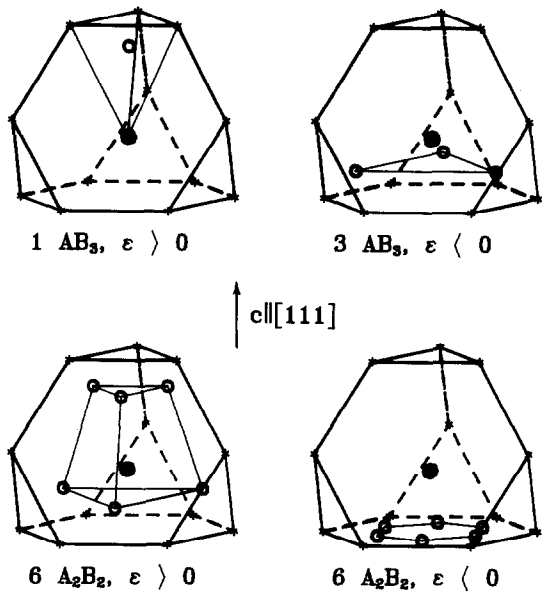

Fig. 8. Friauf polyhedra from B atoms (*) around an A atom (●) and hydrogen sites (○) in both AB_3 and A_2B_2 interstitials at different sign of distortions.

polyhedron contains one hydrogen site, whereas at $\epsilon < 0$ there are three hydrogen sites in one plane. For A_2B_2 interstitials, at $\epsilon < 0$ hydrogen atoms are gathered on one plane which coincides with the plane of M atoms. The distance between hydrogen sites in the plane is $0.19a$, where a is the lattice parameter, and the distance between two neighbouring planes is $0.57a$. Such an anisotropic distribution of hydrogen should increase the negative rhombohedral deformation. At $\epsilon > 0$ the distribution of hydrogen is more isotropic in the volume of the crystal, and additional rhombohedral distortions at the ordering of hydrogen must be smaller.

References

[1] A.V. Korolyov, V.S. Gaviko and N.V. Mushnikov, *Phys. Status Solidi A, 119* (1990) k163.
[2] V.S. Gaviko, A.V. Korolyov and N.V. Mushnikov, *J. Less-Common Met., 167* (1990) 119.
[3] N.V. Mushnikov, A.V. Korolyov, V.S. Gaviko, Ye.I. Raevski and L. Pareti, *J. Appl. Phys., 70* (1991) 2768.
[4] A.V. Korolyov, V.S. Gaviko and N.V. Mushnikov, *IEEE Trans. Magn., 29* (1993) 2899.
[5] A.E. Clark, Magnetostrictive rare earth–Fe_2 compounds, in E.P. Wohlfarth (ed.), *Ferromagnetic Materials*, Vol. 1, North-Holland, Amsterdam, 1980, p. 531.
[6] A.V. Korolyov, N.V. Mushnikov, A.V. Andreev and V.S. Gaviko, *Phys. Met. Metallogr., 2* (1990) 52.
[7] N.V. Mushnikov, V.S. Gaviko and A.V. Korolyov, *J. Alloys Comp., 199* (1993) 61.
[8] V.S. Gaviko, N.V. Mushnikov, A.V. Korolyov, Ye.G. Gerasimov and T.P. Lapina, *Phys. Met. Metallogr., 79* (8) (1994) 167.
[9] D.P. Shoemaker and C.B. Shoemaker, *J. Less-Common Met., 68* (1979) 43.
[10] N.F. Miron, V.N. Scherbak, V.N. Bykov and V.A. Levdik, *Kristallografiya, 16* (1971) 324 (in Russian).

[11] J. Jacob and D. Shaltiel, *J. Less-Common Met., 65* (1979) 117.
[12] D. Fruchart, Y. Berthier, T. DeSaxce and P. Vullet, *J. Less-Common Met., 130* (1987) 89.
[13] B.D. Dunlap, G.K. Shenoy, J.M. Friedt, et al., *J. Appl. Phys., 50* (1979) 7682.
[14] D. Fruchart, Y. Berthier, T. DeSaxce and P. Vullet, *J. Solid State Chem., 67* (1987) 197.
[15] R.R. Birss and G.J. Keeler, *Phys. Status Solidi B, 64* (1974) 357.
[16] M.T. Hutchings, *Advances in Research and Applications (Solid State Physics,* Vol. 16), Academic Press, New York, 1964.
[17] A.J. Freeman and J.P. Desclaux, *J. Magn. Magn. Mater., 12* (1979) 11.
[18] N.V. Kudrevatych, A.V. Deryagin, A.A. Kazakov, V.A. Reimer and V.N. Moskalev, *Phys. Met. Metallogr., 45* (1978) 1169.
[19] N.V. Kudrevatych, V.N. Moskalev, A.V. Deryagin, A.V. Andreev and S.M. Zadvorkin, *Ukr. Fiz. Zh., 26* (1981) 1734 (in Russian).